Kinetics. A ca. 5 μM stock solution of the azoalkane in ethylene glycol or decalin was prepared, containing quinoline or benzophenone as internal standard. The solution was degassed by purging for 15 min with N_2 gas and ca. 5-μL aliquots were transferred into melting point capillaries by means of a syringe, evacuated at water aspirator pressure (ca. 20 Torr) and sealed. Bundles of ca. 20 such tubes were placed into a constant (ca. ±0.15 °C) temperature bath (Fischer Spaltrohrsystem Model 0200/01) at 150–220 °C. After thermal equilibration (ca. 20 min), every 15 min a tube was removed, allowed to cool, and submitted to quantitative capillary gas chromatography, using a 40-m OV-101 column, operated at column, injector, and detector temperatures of 140, 250, and 250 °C, respectively, and a N_2 carrier gas pressure of 1.5 kg/cm^2. Electronic integration against the internal standard afforded the concentration–time data. The rate data were processed according to first-order kinetics to obtain the rate constants and from those the activation parameters according to the Eyring equation. The results are summarized in Table II.

Theoretical Calculations. The enthalpies of formation were calculated by means of the MNDO3 program.[19] All input parameters were optimized and processed without time limit, using an Olivetti M24 personal computer equipped with an arithmetic coprocessor (Intel 8087). The results are summarized in Table III.

Acknowledgment. We thank the Deutsche Forschungsgemeinschaft, the Fonds der Chemischen Industrie, and the Alexander von Humboldt Foundation for generous financial support. For spectral services we are grateful to Dr. G. Lange (MS) and Dr. D. Scheutzow (NMR).

Conformational Properties of the THYME Polyethers. The Bis-THYME Cylinder: A Three-Dimensional Analogue of 18-Crown-6

David M. Walba,*[1] Rodney M. Richards, Mark Hermsmeier, and R. Curtis Haltiwanger

Contribution from the Department of Chemistry and Biochemistry, University of Colorado, Boulder, Colorado 80309-0215. Received January 9, 1987

Abstract: The synthesis and crystal structure of the lowest homologue of the series of macropolycyclic tetrakis(hydroxymethyl)ethylene (THYME) fused-crown ethers, bis-THYME cylinder **5**, are described. Compound **5** was designed as a cylindrical host with a hydrophilic interior surface—a three-dimensional analogue of the "flat" host 18-crown-6. The characterization by X-ray crystallography of the novel trinuclear cascade complex $[K_2(OH_2)\cdot\mathbf{5}]^{2+}[PtCl_3(CH_3)_2SO]_2^-$ (**7**) serves to demonstrate that indeed, at least in the crystalline phase, host **5** does behave as a hydrophilic cylinder and is a remarkably faithful three-dimensional 18-crown-6 analogue. In addition, as the starting point for molecular mechanics study of the THYME polyethers, the free and bound forms of ligand **5** are characterized using MMII and compared with 18-crown-6.

We have recently reported on synthesis of several members of a novel class of molecules composed of crown ether rings fused by the tetrakis(hydroxymethyl)ethylene (THYME) unit.[2] The rationale motivating this project derives from the two separate, though somewhat related, research areas: host-guest chemistry[3] and topological stereochemistry.[4]

In both of these areas, knowledge of the *conformational properties* of the target THYME polyethers is crucially important. In this paper we report experimental details for synthesis of the simplest member of the series, bis-THYME cylinder **5**, details of the crystal structures of two crystalline forms of the material, and the crystal structure of a novel trinuclear cascade complex derived from this host. The results serve as a starting point for exploration of the applicability of the Allenger empirical force-field method[5] for modeling of the THYME polyethers.

Scheme I. Synthesis of the Bis-THYME Cylinder

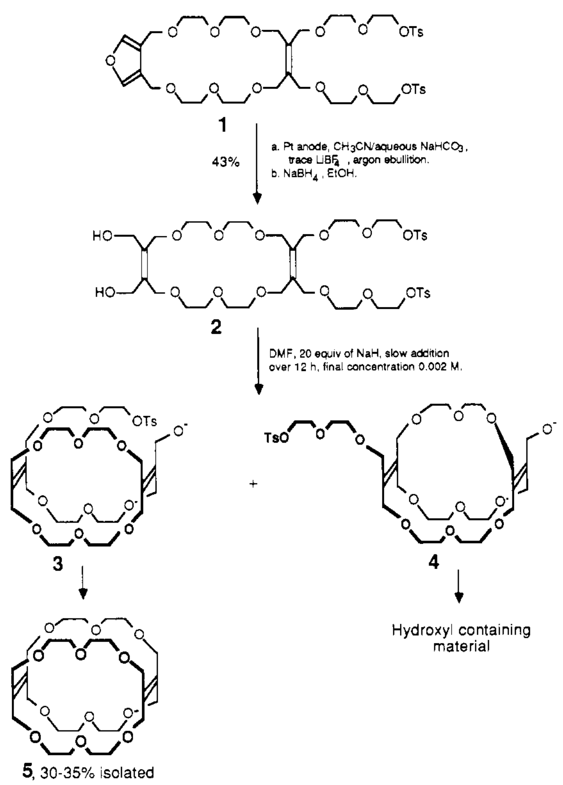

Synthesis of the Bis-THYME Cylinder. From pioneering studies

---

(1) Camille and Henry Dreyfus Teacher–Scholar, 1984–1986.

(2) (a) Walba, D. M.; Richards, R. M.; Sherwood, S. P.; Haltiwanger, R. C. *J. Am. Chem. Soc.* **1981**, *103*, 6213–6215. (b) Walba, D. M.; Richards, R. M.; Haltiwanger, R. C. *J. Am. Chem. Soc.* **1982**, *104*, 3219–3221. (c) Walba, D. M.; Armstrong, J. D., III; Perry, A. E.; Richards, R. M.; Homan, T. C.; Haltiwanger, R. C. *Tetrahedron* **1986**, *42*, 1883–1894.

(3) (a) Cram, D. J.; Cram, J. M. *Science* (*Washington, D.C.* **1974**, *183*, 803. (b) Cram, D. J.; Cram, J. M. *Acc. Chem. Res.* **1978**, *11*, 8–14. (c) Cram, D. J.; Trueblood, K. N. *Top. Curr. Chem.* **1981**, *98*, 43. (d) Lehn, J. M. *Struct. Bonding* (*Berlin*) **1973**, *16*, 1–69. (e) Lehn, J. M. *Pure Appl. Chem.* **1977**, *49*, 857–870. (f) Lehn, J. M.; *Acc. Chem. Res.* **1978**, *11*, 871–892. (g) Vögtle, F.; Sieger, H.; Müller, W. M. *Top. Curr. Chem.* **1981**, *98*, 107. (h) Atwood, J. L., Davies, J. E. D., MacNicol, D. D., Eds. *Inclusion Compounds*; Academic: London, 1984; Vol. 1–3.

(4) (a) Frisch, H. L.; Wasserman, E. *J. Am. Chem. Soc.* **1961**, *83*, 3789. (b) Wasserman, E. *Sci. Am.* **1962**, *107*(5), 94. (c) Schill, G. *Catenanes, Roxtaxanes, and Knots*; Academic: New York, 1971. (d) Sokolov, V. I. *Usp. Khim.* **1973**, *42*, 1037; *Russ. Chem. Rev.* (*Engl. Transl.*) **1973**, *42*, 452. (e) Dmitriev, I. S. *Molecules without Chemical Bonds*; Mir: Moscow, 1981. (f) Walba, D. M. In *Chemical Applications of Topology and Graph Theory*; King, R. B., Ed.; Elsevier: Amsterdam, 1983; pp 17–32. (g) Walba, D. M. *Tetrahedron* **1985**, *41*, 3161–3212.

0002-7863/87/1509-7081$01.50/0 © 1987 American Chemical Society

Table I. Positional and Thermal Parameters for the Nongroup Atoms of Cage **5**·Toluene

atom	x/a	y/b	z/c	$B_{eq}{}^a$ or B, Å^2	atom	x/a	y/b	z/c	$B_{eq}{}^a$ or B, Å^2
O1	0.0726 (5)	0.3392 (4)	0.2563 (4)	5.2	C5	0.1242 (8)	0.3984 (5)	−0.1427 (7)	5.3
O2	0.1117 (5)	0.3459 (4)	−0.0205 (4)	5.1	C6	0.0082 (8)	0.3239 (6)	−0.2585 (7)	6.0
O3	0.0551 (5)	0.2047 (4)	−0.2882 (4)	6.1	C7	0.0107 (7)	0.1120 (6)	−0.2045 (6)	4.8
O4	−0.3001 (5)	0.0669 (4)	−0.3786 (4)	5.2	C8	−0.0421 (7)	−0.0090 (6)	−0.2901 (5)	4.2
O5	−0.3935 (5)	0.1311 (4)	−0.1286 (4)	5.4	C9	−0.1732 (8)	0.0043 (6)	−0.4140 (6)	5.2
O6	−0.2708 (5)	0.1877 (4)	0.1685 (4)	5.5	C10	−0.4036 (8)	−0.0102 (6)	−0.3161 (6)	5.1
C1	−0.0142 (7)	0.1164 (6)	0.2566 (5)	3.8	C11	−0.5006 (7)	0.0682 (6)	−0.2463 (7)	5.3
C2	0.0397 (8)	0.2406 (6)	0.3393 (6)	5.2	C12	−0.4746 (8)	0.1930 (7)	−0.0411 (8)	6.7
C3	0.2192 (8)	0.3301 (6)	0.2117 (7)	5.1	C13	−0.3514 (8)	0.2638 (6)	0.0719 (7)	6.4
C4	0.2189 (7)	0.4072 (6)	0.0947 (7)	5.1	C14	−0.1420 (7)	0.1314 (5)	0.1305 (6)	4.6

[a] B_{eq} is the equivalent isotropic thermal parameter calculated from the anisotropic thermal parameters as $B_{eq} = (B_{11}B_{22}B_{33})^{1/3}$.

on synthetic and semisynthetic host systems,[3] it appears that, in general, the greatest success in molecular recognition is achieved when the host cavity has a high degree of three-dimensionality. In particular, *cylindrical* hosts possess interesting and useful topographic features.

Our plan for synthesis of such hosts is based upon use of the THYME unit as a tetrafunctional linking group. Incorporation of this moiety into cylindrical hosts is considered advantageous for the following reasons: (1) The THYME unit imparts considerable rigidity upon the targets, a property expected to increase selectivity in complexation. (2) The lack of tetrahedral stereocenters in THYME greatly simplifies synthetic considerations. (3) The double bonds present in the target hosts may act as novel binding sites. (4) The double bonds may act as handles for functionalization of the hosts.

The synthesis of bis-THYME cylinder **5**,[2a] proceeds via the furan–crown–ditosylate **1** as shown in Scheme I. Details of the preparation of ditosylate **1** have been reported elsewhere.[2c] Anodic oxidation of this material by the method of Magnusson[6] gives an intermediate bis-hemiacetal, which is immediately converted to the key diol–ditosylate **2** by reduction with sodium borohydride in ethanol.

The strategy now calls for treatment of diol–ditosylate **2** with base under high-dilution conditions. Considering the course of this reaction, it seems the process should proceed in two steps. That is, an initially formed alkoxide will react in an intramolecular sense with one of the two possible tosylate groupings first, and then in a second step the reaction would be completed by coupling of the remaining alkoxide and tosylate groupings. In the initial reaction, two possible regiochemical outcomes are possible. Suppose the "top" alkoxide reacts first. It may attack the top tosylate, leading via a 20-membered ring formation to the alkoxide–tosylate intermediate **3**, which can then cyclize in a second step to the target **5**. However, the top alkoxide seems just as likely to attack the "bottom" tosylate in a 21-membered ring-forming reaction, leading to the regioisomeric "twisted" alkoxide–tosylate **4**.

In this system, examination of CPK models strongly indicates that, once formed, the twisted compound **4** *cannot* undergo a second intramolecular cyclization event. Too much steric strain accrues from such a process. Therefore, this alkoxide–tosylate will either remain unreacted or lead to dimer/polymer via intermolecular couplings. In any reasonable scenario, all products deriving from the twisted initial cyclization mode would possess unreacted hydroxyl functionality. It was therefore assumed that simple alumina chromatography would readily suffice to separate the target polyether cycle **5** from any byproducts.

In fact, cyclization of diol–ditosylate **2** under high-dilution conditions (slow addition of **2** to a suspension of sodium hydride in dry dimethylformamide) followed by removal of solvent at reduced pressure, extractive workup, and chromatography of the crude product on alumina (55% THF/CH_2Cl_2 eluent) gave pure bis-THYME cylinder **5** as a white crystalline solid (mp 118–123 °C) in 30–35% yield.

The physical and spectral properties of host **5** are consistent with the high symmetry (D_{2h}) and tricyclic nature of the molecule. Cylinder **5** is soluble in water, dichloromethane, and chloroform. It is slightly souble in toluene and insoluble in hexane. The EI mass spectrum of **5** shows an abundant molecular ion (16% of the base peak); the ^{1}H NMR spectrum shows the expected AB quartet for the allylic methylene protons (the cylinder cannot "turn inside out") and a broad singlet for the ethyleneoxy protons. The proton-decoupled ^{13}C NMR spectrum shows the expected four unique carbon resonances for the vinyl, allylic, and two heterotopic ethyleneoxy carbons.

Crystal Structure of the Free Ligand. The topology of tricyclic host **5** is unremarkable, being similar to several hosts prepared in recent years.[7-9] From the viewpoint of crown ether chemistry, however, we felt the topography of this host would be interesting to study, since the structure of the molecule is close to a simple "face-to-face" 18-crown-6, possessing two 20-crown-6 rings joined by the rigid THYME unit. It was of some interest to determine whether this host would behave as a three-dimensional analogue of 18-crown-6.

Therefore, single crystals of **5**, suitable for X-ray analysis, were sought. Two crystalline forms, similar to but not identical in conformation of the ligand, were obtained and analyzed as follows.

Crystal Structure of Polyether 5 as the Toluene Solvate. Recrystallization of the chromatographed solid polyether **5** from toluene affords prisms of a 1:1 toluene solvent (**5**·toluene) suitable for X-ray analysis. This solvate loses toluene slowly at room temperature and pressure and rapidly at reduced pressure. After removal of toluene in vacuo, the remaining solid exhibits a melting point identical with that of the chromatographed material.

Compound **5**·toluene crystallizes in space group $P1$: $a = 8.451$ (4), $b = 10.722$ (7), $c = 10.054$ (6) Å; $\alpha = 93.05$ (5), $\beta = 102.59$ (4), $\gamma = 95.33$ (4)°; $V = 882.7$ (8) Å^3; FW = 668.8; $Z = 1$; $D_{calcd} = 1.26$ g/cm^3, $D_{obsd} = 1.29$ g/cm^3; $F(000) = 362$; μ(Mo Kα) = 0.88 cm^{-1}. The structure, solved by direct methods, was refined by full-matrix least-squares calculations, with the disordered solvent treated as a rigid group with individual isotropic thermal parameters. Other nonhydrogen atoms were refined anisotropically. Hydrogen atoms were included in fixed idealized positions with fixed isotropic thermal parameters. For 1091 observed structure amplitudes out of 1730 measured to $2\theta = 40.0°$, the final residuals were $R = 0.056$ and $R_w = 0.070$. The ratio of observations to parameters (194) was 5:1. The estimated standard deviation of an observation of unit weight was 2.09. The maximum shift over error was 0.032 for the disordered toluene. A final electron density difference map showed residual density in the region of the disordered toluene.

Figure 1 shows the crystal structure of **5**·toluene, along with the atomic numbering scheme used in the crystallography. Table

---

(5) Burkert, U.; Allinger, N. L. *Molecular Mechanics*; ACS Monograph 177; American Chemical Society: Washington DC, 1982.

(6) Froborg, J.; Magnusson, G.; Thoren, S. *J. Org. Chem.* **1978**, *43*, 2923–2925.

(7) Lehn has discussed in detail the general properties of cryptate hosts topologically equivalent to bis-THYME cylinder **5** and the formation of binuclear metal complexes with these hosts. See ref 3d,e, and: (a) Lehn, J. M. *Pure Appl. Chem.* **1980**, *52*, 2441–2459. (b) Camarmond, J.; Plumere, P.; Lehn, J. M.; Agnus, Y.; Louis, R.; Weiss, R.; Kahn, O.; Morgenstern-Badarau, I. *J. Am. Chem. Soc.* **1982**, *104*, 6330–6340.

(8) Helgeson, R. C.; Tarnowski, T. L.; Cram, D. J. *J. Org. Chem.* **1979**, *44*, 2538–3550.

(9) Collman, J. P.; Chong, A. O.; Jameson, G. B.; Oakley, R. T.; Rose, E.; Schmittou, E. R.; Ibers, J. A. *J. Am. Chem. Soc.* **1981**, *103*, 516–533.

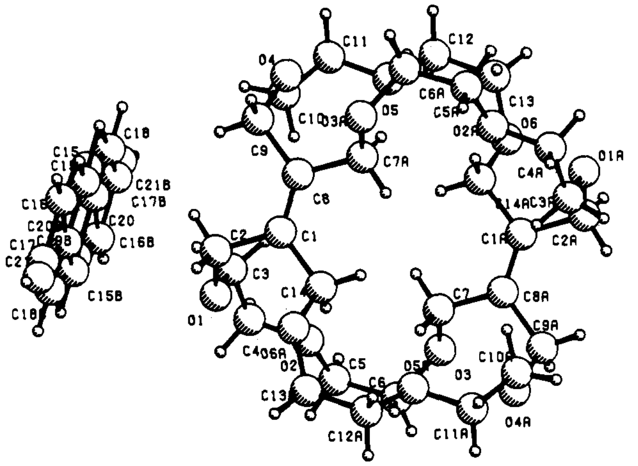

Figure 1. Perspective view and numbering scheme for cage 5·toluene. Atoms labeled A have been generated by the symmetry operation $-x$, $-y$, $-z$.

I gives the positional and thermal parameters for the structure. A stereoview of the unit cell of **5**·toluene is shown in Figure 2 and a stereoview of a single molecule of the polyether in the crystal in Figure 3. As indicated by the ease with which the crystal loses toluene, the aromatic molecule is not strongly associated with molecules of the cage compound.

The polyether adopts a conformation in the crystal, effectively filling the cavity space. The atoms of the cage are located about a center of symmetry, and the two planes defined by the THYME units are parallel but are not perpendicular to the plane defined by the four olefinic carbons. While all of the OCH_2CH_2O units are gauche, four of the eight allylic methylenes are pointing inside the cavity. This structure of the free ligand, as found in the crystal, is schematically represented by the "closed" conformation shown in Scheme II.

Scheme II. Representations of the Two Conformations of Host 5 Found in the Crystal Structures

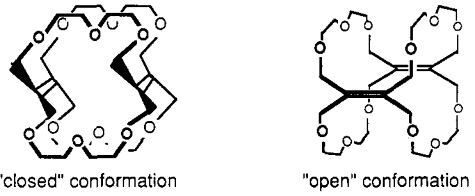

Crystal Structure of Unsolvated Polyether 5. A polymorphic crystal, free of solvent and suitable for X-ray analysis, was grown by diffusion of hexanes into a chloroform solution of host **5**. By this method compound **5** crystallizes in space group $P2_1/c$: a = 8.356 (3), b = 17.029 (8), c = 11.059 (4) Å; α = 90, β = 111.26 (3), γ = 90°; V = 1467 (1) Å^3; FW = 576.68; Z = 2; D_{calcd} = 1.31 g/cm^3, D_{obsd} = 1.29 g/cm^3; $F(000)$ = 624; $\mu(\text{Mo K}\alpha)$ = 0.95 cm^{-1}. The structure, again solved by direct methods, was refined by full-matrix least-squares calculations. All non-hydrogen atoms were refined with anisotropic temperature factors. Hydrogen atoms were included in fixed idealized positions with fixed isotropic thermal parameters. For 1733 observed structure amplitudes out of 3013 measured to 2θ = 50.0°, the final residuals were R = 0.044 and R_w = 0.056. The ratio of observations to parameters (181) was 9:1. The estimated standard deviation of an observation of unit weight was 1.70. The maximum shift over error was 0.005 in the thermal parameters of O1, O2, and C8. A final electron density difference map showed no significant features.

Figure 4 shows the crystal structure of unsolvated **5**, along with the atomic numbering scheme used in the crystallography. Table II gives the positional and thermal parameters for the structure. Again, the free ligand assumes a closed conformation as schematically indicated in Scheme II. This conformation is very similar to, though not identical with, that observed for the toluene solvate.

Preparation and Crystal Structure of the Trinuclear Cascade Complex $[K_2(OH_2)\cdot 5]^{2+}[PtCl_3(CH_3)_2SO]_2^-\cdot CH_2Cl_2$. It is well-

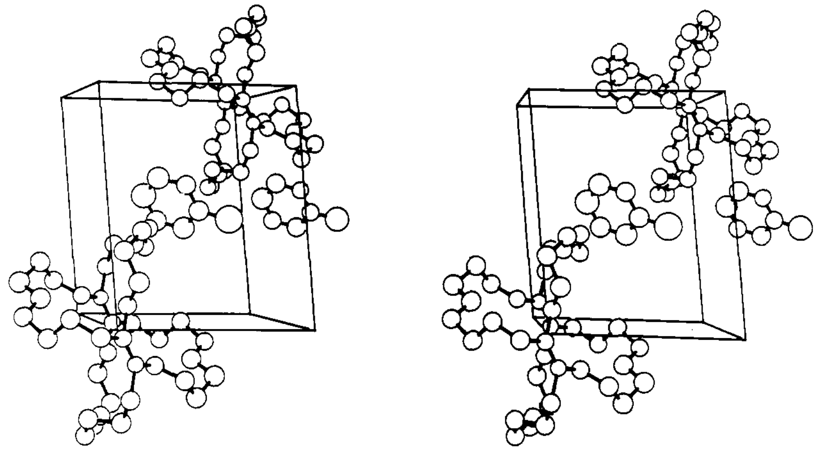

Figure 2. Unit cell diagram for cage 5·toluene.

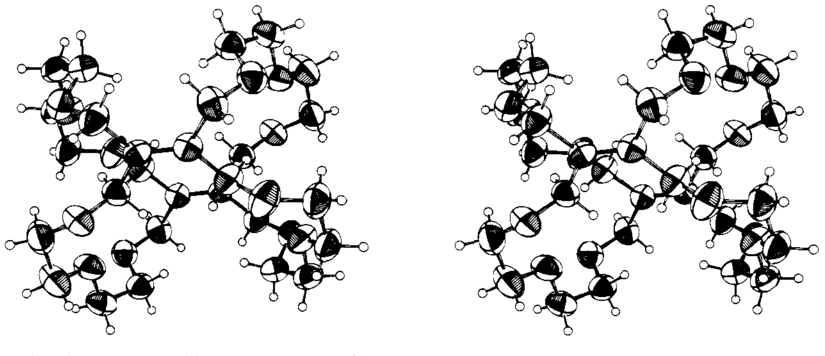

Figure 3. Stereoview of cage 5 showing thermal ellipsoids at the 50% probability level.

Table II. Positional and Thermal Parameters for the Atoms of Cage **5**

atom	*x/a*	*y/b*	*z/c*	$B_{eq}{}^a$ or *B*, Å^2	atom	*x/a*	*y/b*	*z/c*	$B_{eq}{}^a$ or *B*, Å^2
O1	−0.1841 (2)	0.0615 (1)	−0.4086 (2)	4.0	H1C3	−0.312	0.050	−0.294	4.2
O2	−0.1780 (2)	0.1750 (1)	−0.2072 (2)	4.0	H2C3	−0.426	0.072	−0.435	4.2
O3	−0.0438 (2)	0.2143 (1)	0.0702 (2)	4.8	H1C4	−0.415	0.182	−0.326	4.0
O4	0.3519 (2)	0.1785 5(9)	0.2088 (2)	4.1	H2C4	−0.283	0.196	−0.392	4.0
O5	0.3667 (2)	0.1099 (1)	−0.0251 (2)	4.0	H1C5	−0.277	0.262	−0.144	4.1
O6	0.1897 (2)	0.0233 (1)	−0.2639 (2)	4.3	H2C5	−0.159	0.289	−0.217	4.1
C1	−0.0572 (3)	−0.0463 (1)	−0.2629 (2)	2.9	H1C6	−0.018	0.313	−0.006	4.3
C2	−0.1502 (3)	−0.0202 (1)	−0.4011 (2)	3.6	H2C6	0.075	0.243	−0.044	4.3
C3	−0.3198 (3)	0.0813 (2)	−0.3669 (3)	4.1	H1C7	0.082	0.129	0.026	3.6
C4	−0.3090 (3)	0.1657 (2)	−0.3297 (2)	3.9	H2C7	−0.091	0.103	0.034	3.6
C5	−0.1729 (4)	0.2518 (2)	−0.1569 (3)	4.1	H1C9	0.311	0.142	0.362	3.6
C6	−0.0268 (4)	0.2593 (2)	−0.0316 (3)	4.3	H2C9	0.198	0.213	0.295	3.6
C7	0.0069 (3)	0.1346 (1)	0.0722 (2)	3.7	H1C10	0.381	0.066	0.190	3.9
C8	0.0984 (3)	0.1100 (1)	0.2105 (2)	3.0	H2C10	0.547	0.108	0.280	3.9
C9	0.2442 (3)	0.1648 (1)	0.2807 (2)	3.8	H1C11	0.593	0.081	0.097	4.0
C10	0.4496 (3)	0.1120 (2)	0.2020 (3)	4.0	H2C11	0.556	0.171	0.092	4.0
C11	0.5084 (3)	0.1203 (2)	0.0907 (3)	4.0	H1C12	0.493	0.075	−0.132	4.2
C12	0.4105 (3)	0.1142 (2)	−0.1365 (3)	4.7	H2C12	0.456	0.165	−0.141	4.2
C13	0.2539 (4)	0.1008 (2)	−0.2536 (3)	4.6	H1C13	0.281	0.111	−0.328	4.3
C14	0.0832 (3)	0.0098 (1)	−0.1905 (2)	3.3	H2C13	0.167	0.136	−0.251	4.3
H1C2	−0.256	−0.048	−0.435	3.5	H1C14	0.034	0.058	−0.178	3.2
H2C2	−0.081	−0.032	−0.451	3.5	H2C14	0.150	−0.012	−0.109	3.2

[a] B_{eq} is the equivalent isotropic thermal parameter calculated from the anisotropic thermal parameters as $B_{eq} = (B_{11}B_{22}B_{33})^{1/3}$.

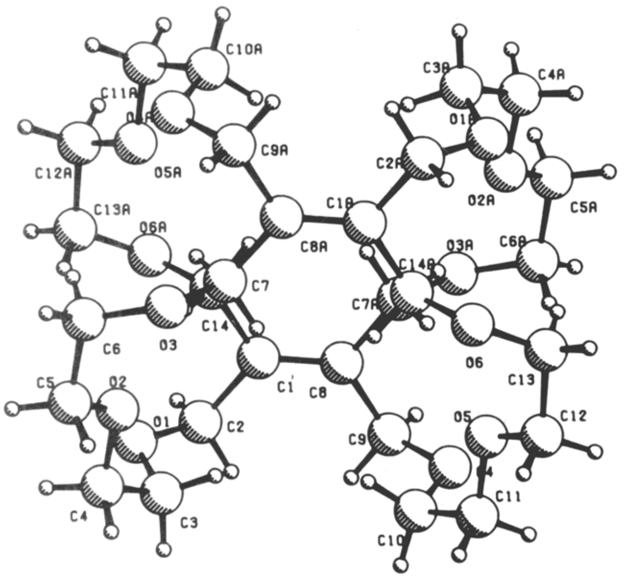

Figure 4. Perspective view and numbering scheme for cage **5**. Atoms labeled A have been generated by the symmetry operation −*x*, −*y*, −*z*.

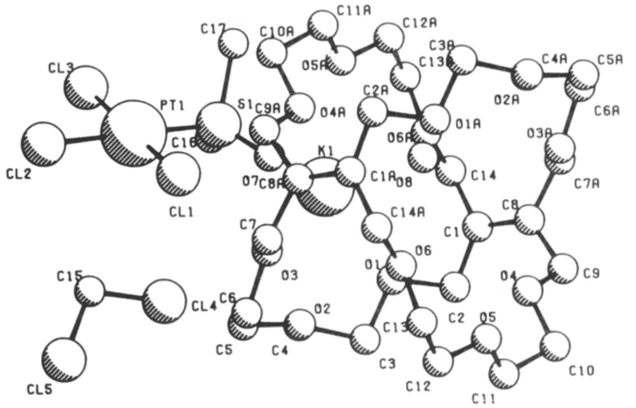

Figure 5. Perspective view and numbering scheme for complex **7**·CH_2Cl_2. The $[PtCl_3DMSO]^-$ anion, the K^+ cation, and the H_2O molecule within the cage are shown in only one symmetry position for clarity. Atoms labeled A have been generated by the symmetry operation −*x*, −*y*, −*z*.

Scheme III. Preparation of the Trinuclear Cascade Complex 7

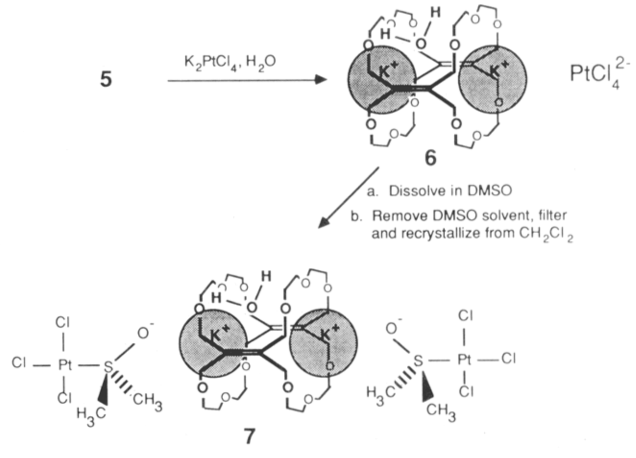

known that often, though a crown ether host will crystallize with no cavity as the free ligand, complexation in solution and in the solid state, nevertheless, occurs. Experiments aimed at demonstrating complexation with ligand **5** were therefore attempted.

Specifically, a solution of host **5** in water was mixed with an aqueous solution of K_2PtCl_4. The solution remained homogeneous at first, but after standing for 12 h at room temperature, opaque salmon-colored needles appeared. This material was insoluble in water and most organic solvents, but dissolved readily in dimethyl sulfoxide (DMSO). The ^1H NMR of a DMSO-d_6 solution of the salmon-colored solid showed very broad signals for the host, indicative of complexation of the polyether ligand in solution.

Removal of DMSO in vacuo followed by trituration of the residue with dichloromethane (CH_2Cl_2), filtration of the resulting suspension (to remove precipitated KCl), and evaporation of solvent gave a yellow semisolid. Crystallization of this material from toluene–CH_2Cl_2 gave clear yellow crystals suitable for X-ray analysis.

The complex crystallizes in space group $P2_1/c$: $a = 10.297$ (6), $b = 25.36$ (2), $c = 12.050$ (4) Å; $\alpha = 90$, $\beta = 113.99$ (4), $\gamma = 90°$; $V = 2873$ (3) Å^3; FW = 1601.77; $Z = 2$, $D_{calcd} = 1.85$g/cm^3, $D_{obsd} = 1.90$g/cm^3; $F(000) = 1572$; μ(Mo Kα) = 58.57 cm^{-1}. The structure, solved by a combination of heavy-atom techniques and direct methods, was refined by full-matrix least-squares calculations. All heavy atoms were refined with anisotropic temperature factors. Hydrogen atoms were included in fixed idealized positions with fixed isotropic thermal parameters. Carbon atoms were refined isotropically. For 1293 observed structure amplitudes out of 3079 measured to $2\theta = 40.0°$, the final residuals were $R = 0.087$ and $R_w = 0.099$. The ratio of observations to parameters (213) was 6:1. The estimated standard deviation of an observation of

Table III. Positional and Thermal Parameters for the Atoms of Complex 7

atom	x/a	y/b	z/c	$B_{eq}{}^a$ or B, Å^2	atom	x/a	y/b	z/c	$B_{eq}{}^a$ or B, Å^2
Pt	0.3769 (3)	0.15501 (9)	0.5463 (2)	4.9	C2	-0.176 (6)	0.140 (2)	-0.150 (5)	5.9
K	-0.106 (2)	-0.0637 (5)	-0.166 (1)	7.9	C3	-0.242 (6)	0.149 (3)	0.012 (5)	7.3
Cl1	0.231 (2)	0.0845 (5)	0.465 (1)	5.2	C4	-0.176 (8)	0.149 (4)	0.148 (7)	11.0
Cl2	0.397 (2)	0.1292 (6)	0.737 (1)	5.2	C5	-0.163 (7)	0.077 (3)	0.284 (6)	8.3
Cl3	0.536 (2)	0.2231 (5)	0.636 (1)	4.5	C6	-0.153 (7)	0.016 (3)	0.306 (5)	7.9
Cl4	-0.011 (3)	0.221 (1)	0.411 (2)	15.4	C7	-0.023 (6)	-0.061 (3)	0.309 (5)	5.7
Cl5	-0.090 (3)	0.212 (1)	0.605 (2)	18.3	C8	0.087 (5)	-0.081 (2)	0.267 (4)	4.2
S	0.356 (2)	0.1814 (6)	0.366 (1)	5.9	C9	0.227 (6)	-0.062 (2)	0.343 (5)	5.3
O1	-0.127 (4)	0.130 (1)	-0.019 (3)	6.3	C10	0.420 (7)	-0.012 (2)	0.333 (6)	7.5
O2	-0.191 (4)	0.090 (2)	0.168 (4)	8.2	C11	0.460 (6)	0.008 (2)	0.235 (6)	6.1
O3	-0.033 (4)	-0.007 (2)	0.289 (4)	8.3	C12	0.412 (6)	0.071 (3)	0.077 (6)	7.5
O4	0.273 (4)	-0.027 (1)	0.269 (3)	4.8	C13	0.326 (6)	0.114 (2)	0.014 (5)	5.8
O5	0.388 (4)	0.051 (2)	0.175 (3)	5.8	C14	0.092 (6)	0.137 (2)	-0.111 (5)	5.4
O6	0.181 (4)	0.098 (2)	-0.038 (3)	6.1	C15	0.051 (9)	0.223 (3)	0.562 (8)	12.5
O7	0.246 (4)	0.162 (2)	0.258 (3)	4.6	C16	0.356 (6)	0.250 (2)	0.357 (5)	6.7
O8	0.088 (9)	-0.011 (4)	-0.005 (7)	7.9	C17	0.535 (5)	0.174 (2)	0.361 (5)	5.7
C1	-0.056 (8)	0.122 (3)	-0.177 (6)	9.2					

[a] B_{eq} is the equivalent isotropic thermal parameter calculated from the anisotropic thermal parameters as $B_{eq} = (B_{11}B_{22}B_{33})^{1/3}$.

Table IV. K^+ Ion Contacts in Complex 7 (Å)

K-O1	3.03 (4)	K-O6	2.99 (3)
K-O2	3.14 (4)	K-O7	2.85 (4)
K-O3	3.04 (4)	K-O8	2.53 (10)
K-O4	2.84 (4)	K-O8′	2.75 (10)
K-O5	2.89 (4)	K-Cl1	3.33 (2)

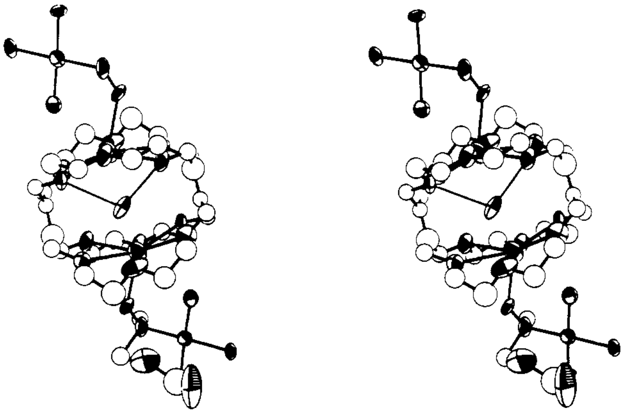

Figure 6. Stereoview of complex 7·CH_2Cl_2. The disordered H_2O within the cage is shown in only one position for clarity.

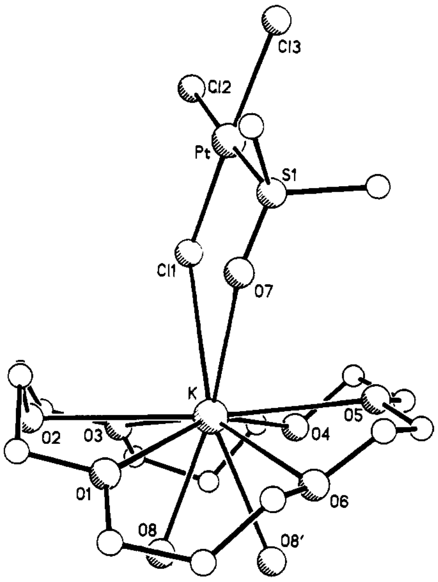

Figure 7. Perspective view of the K^+ coordination sphere.

unit weight was 2.32. The maximum shift over error was 0.014 for C1. The residual peaks in a final electron density difference map are consistent with disorder of the dichloromethane solvate molecule.

These crystals are comprised of a novel trinuclear cascade complex, as shown schematically in Scheme III. Table III gives the positional and thermal parameters for the structure, and the atomic numbering scheme is indicated in Figure 5. A stereoview of the complex is shown in Figure 6. All atoms in the complex are related by a center of inversion. The conformation of the host is an almost idealized "hydrophilic cylinder", as schematically represented by the "open" conformation in Schemes II and III, with all 12 oxygens of the host distributed equidistant from a central axis.

Each 20-crown-6 ring encapsulates a K^+ ion slightly "outside" of the best plane of the six liganding oxygens of the host, and the 20-crown-6 rings pucker considerably to bind the cation. This is readily seen in the detail view of a single 20-crown-6 ring, with it's encapsulated potassium shown in Figure 7. The K^+ contacts in the crystal are given in Table IV. The two potassium nuclei in the complex are separated by 4.91 Å, an extraordinarily close distance for two alkali-metal cations in a binuclear complex. It is interesting to note that the Coulombic repulsion between these two nuclei would be 67 kcal/mol in the absence of the bound water molecule and the atoms of the ligand. A single water molecule is bound within the cavity formed by the two K^+ ions, off the axis and disordered about the inversion center. The shortest metal–oxygen bond distance for the water oxygen is quite short at 2.53 Å.

Interestingly, the Pt moieties are only present as part of the counterions in this complex and are not closely associated with the polyether oxygens or the THYME double bonds. Each of the $PtCl_4{}^{2-}$ anions of the original dipotassium tetrachloroplatinate has exchanged a Cl^- ligand for a DMSO ligand. Thus, there is a $PtCl_3[DMSO]^-$ anion associated with each K^+, bonded via the DMSO oxygen at 2.85 Å. The bond distances and angles of this anion are identical within error with those reported previously for $K^+[Pt(DMSO)Cl_3]$, except for the K–Cl1 interaction, which is significantly longer (3.33 (2) vs 3.224 (6) Å).[10] The potassium cation coordination number is difficult to define. Each potassium cation is within van der Waals bonding distance of six ether oxygens, the sharded water oxygen (disordered in two positions), and the oxygen and a Cl^- from $[DMSO]PtCl_3{}^-$. Finally, dichloromethane solvent molecules are also incorporated in the lattice, though there are no close interactions of the solvent with any components of the complex.

We feel these observations are best interpreted as shown in Scheme III. Thus, treatment of host **5** with aqueous $K_2PtCl_4{}^{2-}$ gives complex **6**, in which the $PtCl_4{}^{2-}$ counterion is intact. It might be noted that, in crystals of this type, a salmon color indicates

---

(10) Melanson, R.; Hubert, J.; Rochon, F. D. *Acta Crystallogr., Sect. B: Struct. Crystallogr. Cryst. Chem.* **1976**, *B32*, 1914–1916.

Table V. Molecular Mechanics Strain Energies (kcal/mol) for Conformations of Bis-THYME Cylinder **5** and for 18-Crown-6

starting conformn of host[a]	E_i[b]	E_f[c]	$E_i - E_f$	E above min[d]
bis-THYME free ligand unsolvated	89.1	70.7	18.4	2.4
bis-THYME free ligand toluene solvate	84.4	70.7	13.7	2.4
bis-THYME cascade complex	145.1	68.3	76.8	0
18-crown-6 free ligand[e]	26.1	21.1	5.0	3.8
K complex of 18-crown-6[e]	19.5	17.3	2.2	0
Rb complex of 18-crown-6[e]	22.6	17.3	5.3	0
Cs complex of 18-crown-6[e]	26.1	17.3	8.8	0
Na complex of 18-crown-6[e]	27.2	23.9	3.3	6.6

[a] The crystal coordinates of the atoms in the ligand for each complex were taken as the starting point for the MMII minimizations. [b] Molecular mechanics energies (relative to an arbitrary zero) obtained by locking in the non-hydrogen atoms of the conformation in the crystal and allowing geometrical optimization of the H atoms. [c] MMII energy of the local minimum found when all atoms of the molecule are allowed to optimize. [d] Difference between the observed energy and the energy of the lowest minimum found. [e] Crystal coordinates obtained from ref 12.

the presence of the tetrachloroplatinate ion. Dissolution of complex **6** in DMSO is accompanied by displacement of chloride by DMSO, and removal of solvent gives a mixture of complex **7**, free ligand, and precipitated KCl. Filtration and crystallization in the presence of dichloromethane then gives rise to the observed material.

Molecular Mechanics Calculations on the Bis-THYME Cylinder. With crystal structure coordinates for three different conformations of the bis-THYME cylinder in hand, we felt it would be interesting to examine this host by the empirical force field method. Thus, the crystal coordinates for the atoms of the *ligand only* for each structure was input and optimized by MMII utilizing Allenger's force fields.[11] The same protocol was followed for several alkali-metal complexes and the free ligand of 18-crown-6 for comparison purposes.[12,13]

The results are shown in Table V. In the table, E_i is the total molecular mechanics strain energy obtained by inputing the X-ray coordinates of the carbon and oxygen atoms of the host and then allowing only the light-atom positions (H) to optimize. Thus, E_i may be considered the MMII energy of the conformation of the host as observed in the crystal structure. Starting with that conformation and allowing a full optimization of all of the atoms of the host then affords an MMII local minimum conformation with strain energy E_f. The difference between these values ($E_i - E_f$) gives an idea, within the MMII model, of how high above the minimum the crystal structure conformation lies.

Finally, for 18-crown-6 three different local minima were found, while for the bis-THYME cylinder two minima were found. The last column in Table I gives the MMII strain energy difference between each conformation and the lowest minimum found for that compound.

Several points concerning the data in Table V deserve comment. First, both crystal conformations of the bis-THYME free ligand optimized to the same local minimum, as expected. A stereoview of this MMII local minimum is shown in Figure 8A. Note that it is very similar to the idealized closed conformation schematically represented in Scheme II. Interestingly, MMII puts the crystal conformation of the unsolvated free ligand higher above the closed local minimum than the conformation observed in the toluene solvate.

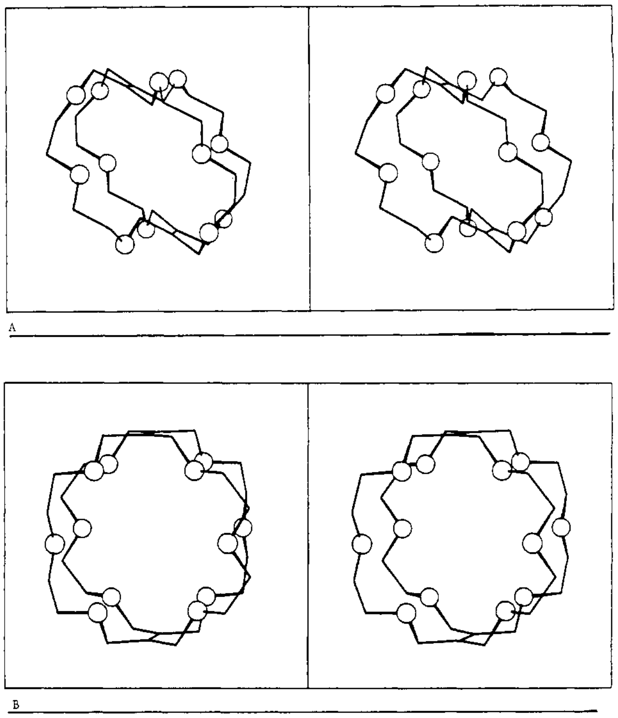

Figure 8. Stereoviews of the MMII local minima for the closed (A) and open (B) conformations.

The conformation of the bis-THYME cylinder found in the trinuclear complex optimized to a different local minimum, as shown in Figure 8B. Note that this conformation is very similar to the idealized open conformation in Scheme II and that this open conformation lies 2.4 kcal/mol lower in energy than the closed conformation. Also, it is interesting that the starting conformation observed in the crystal of the complex lies very high in energy relative to the open local minimum, implying, quite reasonably, that the three guest species are perturbing the conformation to a much greater extent than the crystal lattice interactions in the free ligand.

The behavior of the bis-THYME cylinder is quite similar to that exhibited by 18-crown-6, as indicated by the calculations on the conformations found in the crystal structures of the 18-crown-6 free ligand, sodium, potassium, rubidium, and cesium complexes. The potassium, rubidium, and cesium complex conformations all optimize into the same local minimum, which is the lowest energy conformation found. As for the bis-THYME cylinder, for 18-crown-6 the free ligand conformation optimizes to a local minimum 3.8 kcal/mol higher in energy than the lowest minimum found.

It is easy to speculate on the meaning of the calculations reported in Table V. We have purposefully avoided such speculation since our reason for performing the calculations was to begin exploration of the applicability of the empirical force field method for conformational analysis to the THYME polyethers. It is certainly not clear that the calculations provide an accurate analysis of the conformational surface of such large polyethers. We feel it is important to perform such calculations and present the data obtained, however, since our aim is to determine experimentally whether the calculations are in fact meaningful. In the present study, one may say that the MMII calculations seem to afford reasonable results.

Conclusion

Synthesis of the novel bis-THYME cylinder **5** designed as a cylindrical host with a hydrophilic interior surface—a three-dimensional 18-crown-6—is described. Indeed, the host is shown to behave as a hydrophilic cylinder, at least in the crystalline phase, by characterization of a novel trinuclear cascade complex in which two potassium cations are bound in the 20-crown-6 rings of the

---

(11) Fortran object code for MMII was obtained from the Quantum Chemistry Program Exchange and modified to run on a VAX 11-750 system. The code was also modified to accept 250 atoms, since the QCPE version only allows 100 atoms, and the bis-THYME cylinder possesses 112 atoms (including lone pairs). The ether oxygen force fields used are those of Allenger, as included in the QCPE version of the program.

(12) (a) Bovill, M. J.; Chadwick, D. J.; Sutherland, I. O. *J. Chem. Soc., Perkin Trans. 2* **1980**, 1529. (b) Wipff, G.; Weiner, P.; Kollman, P. *J. Am. Chem. Soc.* **1982**, *104*, 3249–3258.

(13) The crystal coordinates for the 18-crown-6 complexes and the free ligand were obtained from: Dunitz, J. D.; Seiler, P. *Acta Crystallogr., Sect. B: Struct. Crystallogr. Cryst. Chem.* **1974**, *B30*, 2739–2749.

host, serving as binding sites for a single water molecule guest. While the host does not possess a cavity in the conformation observed in crystals of the free ligand, molecular mechanics calculations suggest that perhaps in solution the free ligand of the host does in fact possess a hydrophilic cylindrical cavity.

Experimental Section

Melting points and boiling points are reported in degrees centrigrade and are uncorrected; melting points were determined on a Fisher-Johns melting point apparatus. Infrared (IR) spectra were taken on a Perkin-Elmer Model 727B spectrometer. Proton nuclear magnetic resonance (^{1}H) NMR) and carbon nuclear magnetic resonances (^{13}C NMR) spectra were obtained on a Varian EM 390 (90-MHz) and a Joel PFT (100-MHz) spectrometer, respectively. Chemical shifts are reported in δ downfield from internal standard Me_4Si. Mass spectra were taken at 70 eV on an Atlas MATCH-5 mass spectrometer unless otherwise specified.

X-ray crystallographic data were collected at room temperature with a Nicolet P1 automated diffractometer equipped with a graphite monochromator [μ(Mo Kα) = 0.71069]. Crystals used for data collection were mounted and coated with epoxy resin. Data were collected with variable-speed (2.0–24°/min) θ–2θ scans. The scans were started 0.9° below 2θ for Kα_1 and ended 0.9° above 2θ for Kα_2. Backgrounds were measured at the beginning and end of each scan by using stationary-crystal–stationary-counter techniques. Crystal stability was monitored by measuring four check reflections every 100 measurement cycles. All of the crystals were stable throughout their data collections.

The data were corrected for Lorentz and polarization effects but not for adsorption. Reflections with $F^2 \geq 3.0\sigma(F^2)$ were considered to be significant and were used with weights based on counting statistics for the solution and refinement of the structures. Scattering factors for neutral atoms were used in the refinement. All calculations except the data reduction and direct methods were performed by using the programs contained in the Northwestern University Crystallographic Computing Library of J. A. Ibers. The data reduction program, written in this laboratory, was based, in part, on routines supplied by Syntex Analytical Instruments. The direct-methods program used was MULTAN.[14]

Thin-layer chromatography (TLC) was performed on glass analytical plates (0.2-mm coating, E. Merck silica gel 60 F_{254}) or on alumina plates (alumina 60 F_{254} neutral Type E, E. Merck). Visualization was achieved with either UV light, vanillin spray reagent, or iodine staining. All chromatographic separations were performed on silica gel (40–60 μm, E. Merck) or alumina (alumina Woelm N, by Woelm Pharma, deactivated to grade III with 6% water by weight) by flash chromatography with use of 6 in. of the desired adsorbent. Conditions for separation are reported in parentheses as follows: column diameter, solvent system(s) used for elution, fraction volume, fractions combined for the reported product, R_f in a given solvent system.

Tetrahydrofuran (THF) was purified prior to use by distillation from benzophenone and sodium. Dichloromethane (CH_2Cl_2), acetone, and hexanes were fractionally distilled. Dimethylformamide (DMF) was purified to "super-dryness" by the method of Burfield and Smithers.[15] Reagent-grade methanol, ethanol, and acetonitrile were used without further purification. Reagent pyridine was stored over 3-Å sieves. Dihydropyran (DHP, Aldrich) was distilled from sodium under argon. Sodium borohydride ($NaBH_4$, Alfa) was used without further purification. Oil-free sodium hydride (NaH) was obtained by washing under argon a 50% oil dispersion of NaH (Alfa) several times with hexanes (dried over 3-Å sieves for 48 h) followed by decantation after each washing.

All reactions were stirred magnetically unless otherwise noted.

Reactions requiring an inert atmosphere were run under dry argon. The argon line was arranged such that reaction vessels could be evacuated and purged with argon and then kept under a slight positive pressure of argon with an oil bubbler.

Electrochemical reactions were performed in 50-mL or 100-mL water-cooled beakers with a cylindrical platinum anode (5 cm × 2.8 cm diameter, fine-mesh screen). Argon was bubbled through the reaction mixtures for 10 min prior to and during the period in which current was applied. Supporting electrolyte, $LiBF_4$ (Alfa), was added to obtain a desired voltage.

Elemental analyses were obtained from Galbraith Laboratories, Inc., Knoxville, TN 37921.

20,21-Bis[[2-(2-hydroxyethoxy)ethoxy]methyl]-1,4,7,12,15,18-hexaoxacyclodocosa-9,20-diene-9,10-dimethanol 20,21-Bis(*p*-toluenesulfonate) (2). To a 50-mL electrochemical reaction vessel were added furan **1** (247 mg, 0.247 mmol), 40 mL of acetonitrile, 3.5 mL of saturated aqueous sodium bicarbonate, and enough $LiBF_4$ (~50 mg) to adjust the voltage to 4–5 V at 50 mA. Current was passed through the rapidly stirred mixture until no more starting material was detected by TLC (silica gel, 70% THF/CH_2Cl_2, 60 min or 243 min/mmol). The crude bishemiacetal product was isolated by addition of a trace of hydroquinone, filtration, and evaporation of solvent under reduced pressure. The crude residue was stirred for 12 h at room temperature under argon with 3 mL of ethanol and 20.4 mg (0.54 mmol) of sodium borohydride. The product was extracted from 30 mL of water with CH_2Cl_2 (6 × 30 mL), dried (K_2CO_3/Na_2SO_4), and stripped of solvent under reduced pressure. Chromatography on silica gel (20 mm, 70% THF/CH_2Cl_2, 10 mL, 10–20 plus 100 mL of THF, R_f 0.30 in the same) followed by rechromatography of the mixed fractions in the same manner gave the product diol–ditosylate **2** as a clear colorless oil (109 mg, 43%). ^{1}H NMR ($CDCl_3$) δ 2.45 (s, 3 H), 2.94 (br, 1 H, OH), 3.37–3.38 (m, 14 H), 4.03–4.40 (m, 10 H), 7.30–7.53 (m, 14 H), 7.70–8.00 (m, 2 H); ^{13}C NMR ($CDCl_3$) δ 144.82, 137.93, 136.76, 132.93, 129.82, 127.93, 70.83, 70.69, 69.47, 69.27, 68.60, 67.73, 60.83, 21.60; IR (neat) 3600–3100 (s), 3000–2800 (s), 1660 (w), 1595 (m), 1180–1060 (s) cm^{-1}.

4,7,10,15,18,21,24,27,30,33,36,39-Dodecaoxatricyclo[11.9.9.9^{2,12}]tetraconta-1,12-diene (5). To a stirred argon-protected suspension of oil-free NaH (85.5 mg, 3.56 mmol) in 24 mL of DMF was added, dropwise over 12 hr, a solution of diol–ditosylate **2** (82 mg, 0.089 mmol) in 20 mL of DMF (final concentration of 0.002 M). The suspension was allowed to stir an additional 48 hr at room temperature, solvent was removed by evaporation at reduced pressure, and the residue was dissolved in 30 mL of water. The crude product was isolated by extraction with CH_2Cl_2 (5 × 30 mL), drying (K_2CO_3/Na_2SO_4), and removal of solvent by evaporation under reduced pressure. Chromatography on alumina (20 mm, 55% THF/CH_2Cl_2, 10 mL, 6–20, R_f 0.60 in THF) gave the bis-THYME crylinder **5** as a white crystalline solid: mp 118–123 °C; 16.2 mg, 33%. The product was recrystallized from toluene for single-crystal X-ray analysis. The crystals of toluene solvate were dried in vacuo to obtain the analytical sample. The dried crystals exhibited a melting point identical with that of the chromatographed material. A polymorphic crystal for X-ray analysis was obtained by diffusion of hexanes into a solution of cylinder **5** in chloroform: ^{1}H NMR ($CDCl_3$) δ 3.50–3.83 (br s, 2 H), 4.10, 4.33 (AB qt, 1 H, J = 11.8 Hz, allylic CH_2); ^{13}C NMR ($CDCl_3$) δ 136.58, 71.11, 69.80, 67.95; IR ($CHCl_3$) 3500 (w), 3300 (w), 3250 (w), 3000–2800 (s), 1655 (w), 1460 (w), 1355 (m), 1300 (w), 1135 (m), 1095 (s), 1040 (m), 895 (w) cm^{-1}; mass spectrum, m/e 577 (M^+) 16%. Anal. Calcd for $C_{28}H_{48}O_{12}$: C, 58.22; H, 8.39. Found: C, 58.22; H, 8.36.

Acknowledgment. The following organizations have provided financial support for this work: The Research Corp.; The Petroleum Research Fund, administered by the American Chemical Society; The National Science Foundation (Grant No. CHE-8308087); The Monsanto Agricultural Products Co. We are especially indebted to the Office of Naval Research for partial support of this work.

Registry No. 1, 79289-90-0; **1** (bishemiacetal), 110512-25-9; **2**, 110512-26-0; **5**, 110512-27-1; **5**·toluene, 110512-28-2; $[K_2(OH_2)\cdot\mathbf{5}]^{2+}\cdot[PtCl_3(CH_3)_2SO]^{-}\cdot CH_2Cl_2$, 110570-47-3.

Supplementary Material Available: Tables of anisotropic thermal parameters, group parameters for the toluene solvate, hydrogen atom parameters, bond distances, bond angles, and torsion angles (11 pages); observed and calculated structure factor amplitudes for all three crystal structures reported (14 pages). Ordering information is given on any current masthead page.

---

[14] Germain, G.; Main, P.; Woolfson, M. M. *Acta Crystallogr., Sect. A: Cryst. Phys., Diffr., Theor. Gen. Crystallogr.* **1971**, *A27*, 368–376.

[15] Burfield, D. R.; Smithers, R. H. *J. Org. Chem.* **1978**, *43*, 3966–3968.